*Proceedings of the 20th International Conference on Soil Mechanics and Geotechnical Engineering– Rahman and Jaksa (Eds)*


# An automated image-based technology for soil 3D deformation measurement and constitutive parameters derivation

## Une technologie automatisée basée sur l'image pour la mesure de la déformation 3D du sol et la dérivation des paramètres constitutifs

**Zewen Wang**, Wenhan Du, James Doherty & Barry Lehane
*University of Western Australia, Perth WA, Australia, zewen.wang@research.uwa.edu.au*

Stanier Sam
*University of Cambridge Cambridgeshire, United Kingdom*

David White
*University of Southampton, Southampton, United Kingdom*

Qingbing Liu
*China University of Geosciences, Wuhan Hubei Province, China*

ABSTRACT: This paper describes a new automated method developed at the University of Western Australia (UWA) of obtaining accurate and objective measurements of the stiffness of triaxial soil samples. The vertical and lateral movements of the patterned membrane on the surface of the triaxial specimen are determined using digital image correlation and 3D photogrammetry of images obtained using 16 No. (inexpensive) Raspberry pi cameras mounted outside the Perspex wall of the triaxial cell. These measurements are combined with the internal load cell records and then processed in a format that allows the degradation of stiffness with axial and radial strain as well as other conventional triaxial test data. The paper describes the procedures and set of essential corrections required to ensure maximum resolution of axial and radial strain. The current resolution is shown to be 0.002mm which is sufficiently small to dispense with local strain gauges and bender elements for most practical applications. This triaxial system, which is easily adapted at low cost to most existing commercial triaxial testing machines, is combined with UWA software that allows derivation of soil parameters for a range of constitutive soil models.

RÉSUMÉ: Cet article décrit une nouvelle méthode automatisée développée à l'Université de l'Australie occidentale (UWA) pour obtenir des mesures précises et objectives de la rigidité d'échantillons de sol triaxiaux. Les mouvements verticaux et latéraux de la membrane à motifs sur la surface de l'échantillon triaxial sont déterminés à l'aide de la corrélation d'images numériques et de la photogrammétrie 3D des images obtenues à l'aide de 16 caméras Raspberry pi (bon marché) montées à l'extérieur de la paroi en Perspex de la cellule triaxiale. Ces mesures sont combinées avec les enregistrements de la cellule de pesée interne, puis traitées dans un format qui permet la dégradation de la rigidité avec des déformations axiales et radiales ainsi que d'autres données d'essai triaxiales conventionnelles. Le document décrit les procédures et l'ensemble des corrections essentielles nécessaires pour assurer une résolution maximale de la déformation axiale et radiale. La résolution actuelle est de 0,002 mm, ce qui est suffisamment petit pour se passer de jauges de contrainte locales et d'éléments de cintrage pour la plupart des applications pratiques. Ce système triaxial, qui est facilement adapté à faible coût à la plupart des machines d'essai triaxiales commerciales existantes, est combiné avec le logiciel UWA qui permet de dériver des paramètres de sol pour une gamme de modèles de sols constitutifs.

KEYWORDS: Triaxial test, 3D photogrammetry, digital image correlation, numerical analysis

## 1 INTRODUCTION

All civil engineering design and construction requires knowledge of the mechanical properties of the foundation soil. The high non-linearity of soil stiffness even at strains as low as 0.005% makes the stiffness difficult to measure and characterize (Jardine et al. 1986). Current laboratory testing and interpretation methods still involve low-technology procedures and subjective assumptions, which hamper the development of efficient engineering design methods and constitutive models (Lehane et al. 2009, Doherty et al. 2017). Given the importance of measuring stiffness non-linearity and using realistic constitutive models in engineering design, several local strain measurement techniques have been developed to measure strain on triaxial samples to provide the necessary stiffness data. These approaches have a clear advantage over conventional strain measurement using external displacement transducers, but they are expensive and cumbersome, and require skilled operators.

With ongoing developments of digital cameras, the image analysis approach to measure deformation of triaxial soil samples has become feasible and cost-effective. Some other benefits of the image analysis approach include ease of installation and no contact with the specimen under test. Particle image velocimetry (also known as digital image correlation) is one image analysis

approach that has been used for a variety of geotechnical applications in the laboratory, centrifuge, and field (White et al. 2001; Rechenmacher and Finno 2003; Iskander 2010; Bhandari 2011; Hall 2012; Stanier et al. 2015). However, a limitation of most PIV approaches is that they only provide planar or two-dimensional (2-D) information. In a triaxial test, the soil specimen experiences axial and radial deformations during shearing, and movements cannot be effectively distinguished from 2-D images. For example, as illustrated in Figure 1, the radial deformation pushes the sample edge towards the camera and indicates an apparent vertical movement of subsets on the image plane.

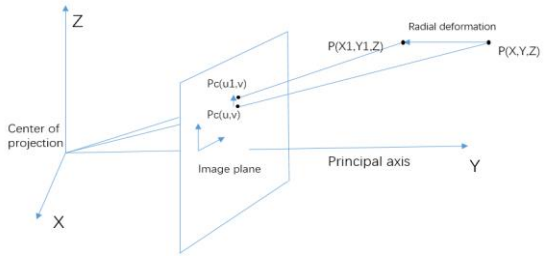


Figure 1: Pinhole camera model

Limited studies of three-dimensional (3D) PIV have been reported in the geotechnical literature (Taylor et al. 1998; OROZCO n.d.; Zhang et al. 2015). These studies do not target the small deformation and are expensive to set up.

This paper presents a component of a larger research project on cost-effective soil parameter determination and introduces a 3D image analysis approach proposed for triaxial testing. This is specifically designed for accurate measurement of the 3D displacements of the external membrane of a cylindrical triaxial soil sample. The proposed method does not require the modification of a conventional triaxial testing system. The equipment used for this method has an overall cost of about A$2800, which is considerably cheaper than the cost of bender elements and local strain gauges. Hence, it is hoped to find application in many laboratories around the world.

## 2 EXPERIMENTAL SET-UP

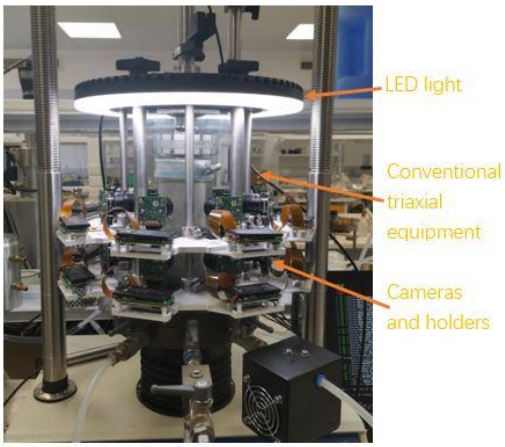


Figure 2: Application of proposed method to triaxial testing

Figure 2 shows an example application of the proposed testing technique on a 63mm diameter, 140mm high triaxial specimen. The particular application shown involves the use of 16 cameras which provide full coverage of the entire surface of the cylindrical triaxial test soil specimen. An LED light is mounted on top of the triaxial cell to improve the image quality with sufficient light. The number of cameras used can be changed for a different size of triaxial specimens and chambers.


Figure 3: Cameras & camera holders

Each of the cameras is composed of a raspberry pi zero board, a raspberry pi HQ camera, a 6mm wide-angle lens, and a lithium battery (Figure 3). The HQ camera is capable of taking 12.3 megapixels' images and has a low cost compared to other commercial cameras. The 6mm lens can handle extremely close focusing distances, and therefore allows the camera to be placed just outside the triaxial chamber. The camera does not support auto-focus and requires the user to manually adjust and fix the focus at the beginning of the test. Each raspberry pi board is charged by a lithium battery and connected to a HQ camera to control the camera and store the images. All raspberry pi boards are connected to a local desktop through a local Wi-Fi network. The desktop PC controls the raspberry pi's to capture images synchronously and transfer captured images after each test. All wire connections are removed to avoid disruption to the camera. Each battery can be re-charged or replaced without disruption to the system.

Eight 3D-printed camera holders are used to fix the positions of all the cameras to the (six) vertical bars that tie together the upper and lower ends of the triaxial chamber (see Figure 2). The camera holders (see Figure 3) are designed to make sure that every two adjacent cameras have appropriate overlaps of the respective fields of view.

The accuracy of PIV analysis depends on attaining sufficient contrast between areas in the image. A speckle pattern on the traditional non-porous latex membrane is created by spraying it with black paint; this process is completed in a matter of minutes and adds contrast and improves the accuracy of PIV analysis (Figure 4). As for any triaxial test, the properties of the membrane have an insignificant effect on the measured stress - strain characteristic except at very large strains in extension tests (Head 2006).

Figure 4: Speckle painted non-porous latex membrane

A target in the form of a perfect cylinder with similar dimensions to the soil sample being tested is required to calibrate all the cameras (Figure 5a). The traditional planar target is not used as it does not allow multiple cameras to observe the same location on elements of the target. A calibration pattern printed on vinyl paper with a protective varnish and an adhesive backing, shown on Figure 5b, is fixed to the surface of the cylinder and

placed in the triaxial apparatus. The calibration is performed when the triaxial cell is filled with water.

The optimal calibration pattern, which was selected after a number of trials, combined Aruco markers with a grid of circles. As shown in Figure 6, the Aruco marker is a synthetic square marker with a black border that can be detected rapidly and an inner binary matrix that defines its identification. The detection of the border of the Aruco marker is not sufficiently accurate. However, the centre of adjacent circles can be detected and their coordinates can be refined more accurately. The Aruco markers are therefore used is to allow identification of the circles. The centers of the circles are extracted for calibration.

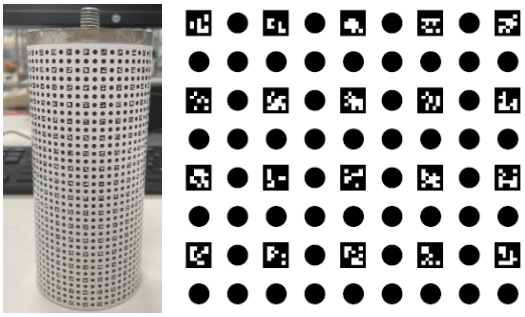

Figure 5: (a) Calibration target (b) Calibration pattern (Aruco marker & circle grid)

The procedure followed in the triaxial testing performed to date is as follows:

1) Attach all cameras and the holders to the triaxial chamber and fix their positions.
2) Manually adjust the focus of each camera to obtain optimal image quality and then fix the focus.
3) During the shearing stage of the triaxial test, control all cameras to capture images simultaneously at each time interval.
4) After the test is completed, remove the soil sample and place the calibration target into the triaxial chamber, and attach the ram to the calibration cylinder so that it can be rotated a little from outside the cell.
5) Fill the cell with water and increase the cell pressure to the value using in the test.
6) Control all cameras to take a calibration image simultaneously.
7) Rotate the calibration target by about 5 degrees and take another set of calibration image from a different view. Repeat this process several times.
8) Input all taken images into a written image analysis program, which performs the image analysis automatically.

## 3 PHOTOGRAMMETRY

This section introduces the image analyzing procedure of the proposed method, which can be divided into 3 steps, namely (i) camera calibration, (ii) subset selection and tracking and (iii) 3D reconstruction.

### 3.1 *Camera calibration*

The photogrammetry used is based on the concept of the pinhole camera model (see Figure 1) which describes the relationship between the 3D coordinate of a point on the soil sample surface and its projection on the image plane. A simple relationship between an object's 3D real-world coordinate (X, Y, Z) and its corresponding image coordinate is as follows:

$$s\begin{bmatrix} u \\ v \\ 1 \end{bmatrix} = \begin{bmatrix} fx & 0 & cx \\ 0 & fycy & \\ 0 & 0 & 1 \end{bmatrix} [R|T] \begin{bmatrix} X \\ Y \\ Z \\ 1 \end{bmatrix} \quad (1)$$

Where:

- (u, v) are the coordinates of the projection point in image coordinate (pixels)
- $\begin{bmatrix} fx & 0 & cx \\ 0 & fycy & \\ 0 & 0 & 1 \end{bmatrix}$ is the camera matrix (intrinsic parameters)
- $[R|T]$ are the extrinsic parameters
- R: Rotation matrix
- T: Translation vector

The camera calibration determines the relationship between two coordinate systems by estimating the camera's intrinsic and extrinsic parameters using calibration images taken at steps 5 and 6 above. For each image, the image coordinate of all circle centres is first detected by the image analysis program (see Figure 6). The 3D coordinate of all detected centres is first calculated according to the dimension of the calibration target. The intrinsic and extrinsic parameters for each camera are then estimated using the method introduced by Zhang (2000). The intrinsic parameters contain information relating to the optical centre and focal length of the camera and do not depend on the scene viewed. Extrinsic parameters represent the location of each camera in the 3D scene. Each calibration image is taken from a different view and generates multiple extrinsic parameters. For each camera, multiple calibration images are used to improve the overall accuracy of the estimated intrinsic parameters, but only the extrinsic parameters calculated from the image taken at Step 5 are selected as this camera's extrinsic parameters.

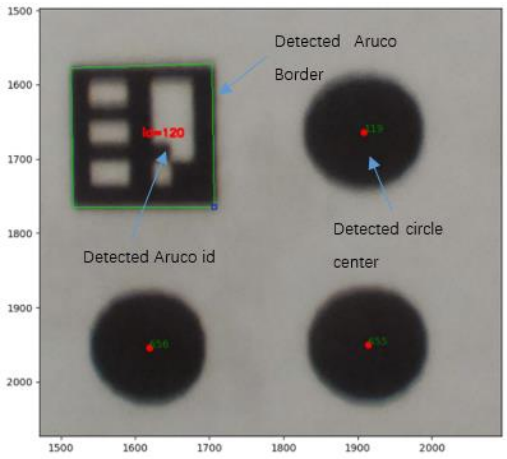


Figure 6: Marker and circle detection

The calibration procedure also calculates each camera's distortion parameters. The camera matrix in equation 1 does not include the lens distortion as an ideal pinhole camera model does not have a lens. Distortion parameters are used to correct the distorted image coordinate (u, v) caused by the bending light rays and slight deviations from parallel orientations of the lens and image plane. It is assumed that the estimated distortion parameters from camera calibration also account for the refraction at the interface between cell fluid and curved cell wall since the calibration image is taken when the calibration target is placed inside the triaxial chamber.

### 3.2 *Subsets selection and subsets tracking*

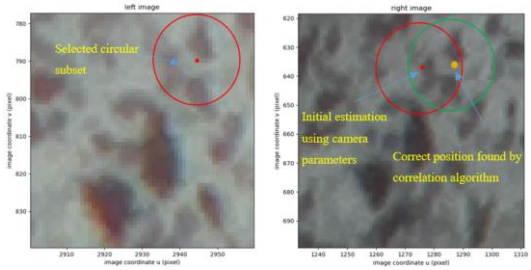


Figure 7: Subset selection

3D deformation data are obtained by tracking the 3D coordinates of several interest points during the shear stage. A group of interest points is selected within the overlapping area of two horizontally adjacent cameras. Subsets on the reference image are defined first and the PIV analysis finds correlated subsets on the consecutive images. Subsets are a group of uniquely colored pixels shown on an image that PIV can track during the deformation process. The subsets shown on the reference images which represent the projection of selected interest points are estimated by first using camera parameters. As shown in Figure 7, the image coordinate of subsets on reference images of two cameras is further refined by using a correlation algorithm to make sure that PIV tracks the same subsets on two sets of camera's view.

The PIV analysis uses GeoPIV_RG described by Stanier et al. (2015). For each camera, the GeoPIV_RG tracks the defined subsets on the consecutive images. The output is the image coordinate of selected subsets from each image.

### 3.3 *3D reconstruction*

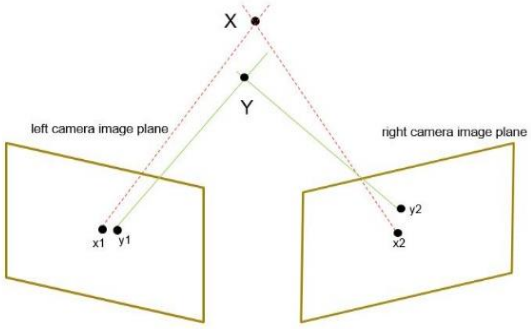


Figure 8: Concept of triangulation

For each pair of cameras, the 3D reconstruction calculates the 3D coordinate of the interest points based on the subsets tracking results from two cameras. This process is also referred to as triangulation in computer vision which finds the 3D coordinate of a point by finding the intersection (X in Figure 8) of the two projection rays. The projection rays (dotted line in Figure 8) can be determined based on its corresponding image coordinate (x1, x2) and camera parameters. The triangulation method used in this research is the direct linear transformation algorithm introduced in Hartley (2004). In practice, two points may not intersect or intersect at the wrong place (Y in Figure 8). This is caused by the inaccurate measurement of image coordinate (y1, y2) due to distortion. Therefore, the image coordinate data obtained from PIV analysis is first corrected by applying the distortion parameters before triangulation.

The output data are the 3D coordinates of the selected subsets during the entire shear stage, which allows accurate measurement of axial and radial strain under triaxial conditions. Researchers and engineers can use these measurements to derive the constitutive parameters they need.

## 4 TYPICAL RESULTS

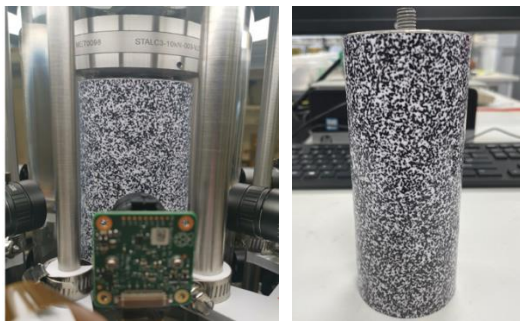

Figure 9: (a) Setup of the dummy sample test (b) Dummy sample

A stainless steel dummy sample wrapped with a random pattern was used to validate the developed system. As shown in Figure 9, the dummy sample is fixed to the loading frame by attaching to the load cell ram. During the test, cameras move with the triaxial chamber and have a relative movement with the dummy sample. An LVDT is placed on top of the chamber to measure the vertical movement. The chamber moved with a constant speed of 0.01 mm per minute and the images were taken every 30 seconds. The average vertical displacement measured from all interest points using the proposed method and the result from LVDT is shown in Figure 10. The difference between the two measuring approaches is found to be 0.00018 +0.00075 mm.

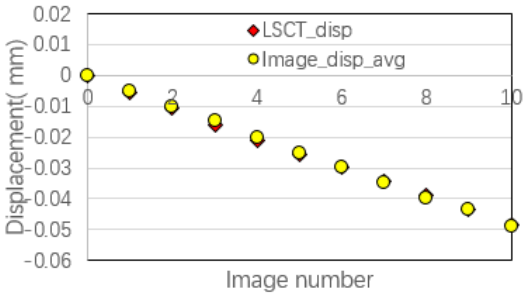


Figure 10: Displacement measurement using two approaches

To demonstrate the application of the developed approach to an actual soil test, a drained triaxial compression test was performed on a sample of fine silica sand that was initially consolidated to an axial effective stress 82 kPa and radial effective stress of 50 kPa. The specimen had a diameter of 62.7 mm and an initial height of 139.5mm and was sheared to an axial strain of 0.1% with a constant speed of 0.0023 mm/min. During the test, images were captured and analyzed following the procedures outlined above.

The local axial strain was calculated as the average of 2 subsets of 3D coordinate data derived from image analysis. These strains are plotted on Figure 11 which compares the deviator stress vs. axial strain measurement and the corresponding smoothened Young's modulus (E'v) data determined from image analysis and external LVDTs. A much stiffer initial response is predicted for the sample using the image analysis strain data. This stiffer response is in line with the anticipated degradation of stiffness inferred from correlations presented in Lehane & Cosgrove (2000). The smaller stiffness inferred from the LVDT data arises due to factors such as compliance in the triaxial apparatus, as described by Jardine et al. (1986). The image analysis data indicate higher stiffnesses

than expected at very low strains (less than 0.005%) and highlights the need for improved resolution at very low strains. The accuracy is influenced by (a) the image quality, (b) the error of matched subsets from two adjacent cameras, and (c) the error of camera calibration. These and other issues are the subject of ongoing research.

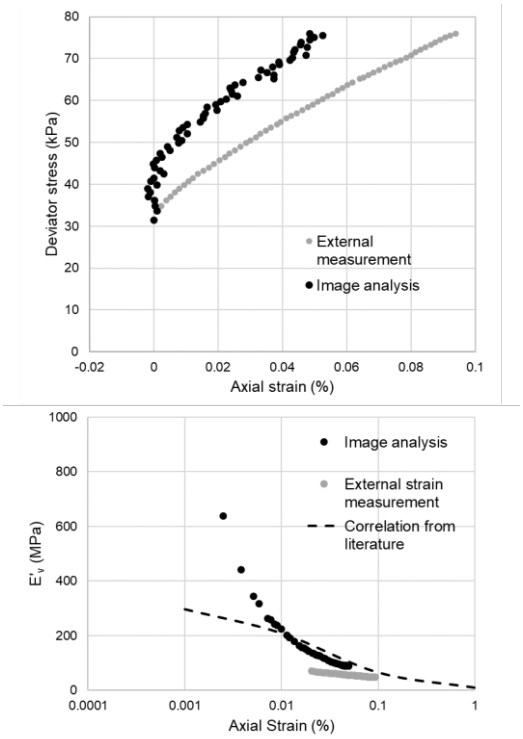


Figure 11: A comparison of triaxial data for axial strain measurements determined using image analysis and an external displacement transducer

## 5 CONCLUSIONS

The paper presents a new automated image analysis method that can be applied to conventional triaxial equipment to provide accurate deformation measurement in both static and cyclic tests and hence stiffness during tests. The image analysis is fully automated and the cost of the system is low relative to the cost of other local strain measurement devices. It is shown that the strain resolution is of the order of 0.005% and this is likely to improve as the research efforts continue.

## 6 REFERENCES


Bhandari, A. R., Powrie, W., & Harkness, R. M. (2011). A digital image-based deformation measurement system for triaxial tests. Geotechnical Testing Journal, 35(2), 209-226.

Doherty, J. P., Gourvenec S. & Gaone F. (2017a). Insights from a shallow foundation load-settlement prediction exercise (Computers and Geotechnics).

Jardine, R.J., Potts, D.M., Fourie, A.B. and Burland, J.B., 1986. Studies of the influence of non-linear stress–strain characteristics in soil–structure interaction. Geotechnique, 36(3), pp.377-396.

Hall, S.A., 2012. Digital image correlation in experimental geomechanics. ALERT Geomaterials Doctoral Summer School, pp.69-102.

Hartley, R. and Zisserman, A. (2004) "Structure Computation," in Multiple View Geometry in Computer Vision. 2nd edn. Cambridge: Cambridge University Press, pp. 310–324. doi: 10.1017/CBO9780511811685.017.

Head, K. H. (2006). Manual of soil laboratory testing (Vol. 1). Manual of Soil Laboratory Test.

Iskander, M., and Liu, J., 2010. Spatial deformation measurement using transparent soil. Geotechnical Testing Journal, 33(4), pp.314-321.

Lehane, B. and Cosgrove, E., 2000. Applying triaxial compression stiffness data to settlement prediction of shallow foundations on cohesionless soil. Proceedings of the Institution of Civil Engineers-Geotechnical Engineering, 143(4), pp.191-200.

Lehane B.M., Doherty J.P. and Schneider J.A. (2009). Settlement prediction for footings on sand. Keynote Lecture, Proc. 4th International Symposium on deformation characteristics of Geomaterials, Atlanta, 1, 133-152, IOS press, The Netherlands.

OROZCO, V.J.C., A Simplified 3D Soil Deformation Measurement under Uniaxial Compression Test via PIV and Stereophotogrammetry.

Rechenmacher, A.L., and Finno, R.J., 2003. Digital image correlation to evaluate shear banding in dilative sands. Geotechnical Testing Journal, 27(1), pp.13-22.

Stanier, S. A., Blaber, J., Take, W. A., & White, D. J. (2015). Improved image-based deformation measurement for geotechnical applications. Canadian Geotechnical Journal, 53(5), 727-739.

Taylor, R.N., Grant, R.J., Robson, S., and Kuwano, J., 1998. An image analysis system for determining a plane and 3-D displacements in centrifuge models. Balkema.

White, D. J., Take, W. A., & Bolton, M. D. (2001, September). Measuring soil deformation in geotechnical models using digital images and PIV analysis. In International Conference on Computer Methods and Advances in Geomechanics (No. 10, pp. 997-1002).

Zhang, Z., 2000. A flexible new technique for camera calibration. IEEE Transactions on pattern analysis and machine intelligence, 22(11), pp.1330-1334.

Zhang, X., Li, L., Chen, G. and Lytton, R., 2015. A photogrammetry-based method to measure total and local volume changes of unsaturated soils during triaxial testing. Acta Geotechnical, 10(1),